J|A|C|S
ARTICLES
Published on Web 06/04/2004

Generation and Photoreactions of 2,4,6-Trinitreno-1,3,5-triazine, a Septet Trinitrene

Tadatake Sato,*[,†] Aiko Narazaki,[†] Yoshizo Kawaguchi,[†] Hiroyuki Niino,[†] Götz Bucher,*[,‡] Dirk Grote,[‡] J. Jens Wolff,[§,⊥] Hans Henning Wenk,[‡] and Wolfram Sander[‡]

Contribution from the Photonics Research Institute, National Institute of Advanced Industrial Science and Technology (AIST), 1-1-1 Higashi, Tsukuba, Ibaraki 305-8565, Japan, Lehrstuhl für Organische Chemie der Ruhr-Universität Bochum, Universitätsstrasse 150, D-44801 Bochum, Germany, and Institut für Organische Chemie, Ruprecht-Karls-Universität Heidelberg, Im Neuenheimer Feld 270, D-69120 Heidelberg, Germany

Received December 18, 2003; E-mail: sato-tadatake@aist.go.jp; goetz.bucher@ruhr-uni-bochum.de.

Abstract: We have studied the matrix photolysis of 2,4,6-triazido-1,3,5-triazine (cyanuric triazide, **1**). Stepwise generation of the corresponding mononitrene, dinitrene, and trinitrene was observed by matrix IR and electron paramagnetic resonance (EPR) spectroscopy. The generated species were identified by comparison of their matrix IR spectra with density functional theory (DFT) computational results. The generation of 2,4,6-trinitreno-1,3,5-triazine with a septet ground state was confirmed for the first time by matrix EPR spectroscopy. The trinitrene readily decomposed into three NCN molecules upon further photoirradiation. This process was also confirmed by matrix EPR spectroscopy.

Introduction

In the past decade, high-spin oligonitrene species have been widely studied as model systems for organic magnetism and molecular-spin science.[1] The chemistry of oligonitrenes under matrix photolysis conditions is often complex because of the facile rearrangement of arylnitrenes to bicyclic azirines and azacycloheptatetraenes.[2] Such rearrangements are frequently suppressed by the introduction of *ortho* substituents[3−5] or the replacement of the *ortho* carbon by nitrogen.[6−8] For instance, Chapyshev et al. recently succeeded in generating a septet trinitrene species from a substituted pyridine system.[9]

2,4,6-Triazido-1,3,5-triazine (cyanuric triazide, **1**) has been studied as a potential precursor of a high-spin trinitrene molecule. In 1966, Moriarty, Rahman, and King described the cryogenic matrix photolysis of **1**, in which only a mononitrene signal was observed.[10] They estimated the fine-structure D parameter of the nitrene as $D = 1.440$ cm^{-1} and suggested the generation of NCN on the basis of the unexpected large D value. In a later reinvestigation, the generation of a triplet mononitrene and a quintet dinitrene upon photolysis of a single crystal of **1** at 4 K was confirmed by electron paramagnetic resonance (EPR) spectroscopy. The fine-structure D and E parameters of the mononitrene were estimated as 1.402 and 0.011 cm^{-1}, respectively. The generation of a septet trinitrene was not, however, reported.[11] In that study, the oligonitrene species generated were surrounded by the unreacted precursor or by partially reacted nitrenes. Even at 4 K, reactions between these species could not be excluded completely. On the other hand, the matrix-isolation technique using inert media such as noble gases or nitrogen allows the study of such reactive species by excluding intermolecular reactions completely. Recently, we reported on the formation of a trinitrene upon photolysis of **1** isolated in a nitrogen matrix.[12] In this Article, we describe a detailed study of the photolysis of **1** in nitrogen matrixes by using Fourier transform infrared (FTIR), ultraviolet−visible (UV−vis), and EPR spectroscopy.

Experimental Section

I. Matrix Photolysis: FTIR and UV−Vis Absorption Measurements. 2,4,6-Triazido-1,3,5-triazine (**1**) was synthesized by mixing an acetone solution of cyanuric chloride (2,4,6-trichloro-1,3,5-triazine) with

[†] National Institute of Advanced Industrial Science and Technology.
[‡] Lehrstuhl für Organische Chemie der Ruhr-Universität Bochum.
[§] Ruprecht-Karls-Universität Heidelberg.
[⊥] Deceased.

(1) Nimura, S.; Yabe, A. In *Molecular Magnetism of Organic Molecules and Materials;* Lahti, P. M., Ed.; Marcel Dekker: New York, 1999; pp 127−146, and references therein.
(2) Wentrup, C. *Reactive Molecules. The Neutral Reactive Intermediates in Organic Chemistry*; Wiley: New York, 1984; pp 212−221.
(3) Dunkin I. R.; Thomson, P. C. P. *J. Chem. Soc., Chem. Commmun*. **1982**, 1192−1193.
(4) Dunkin I. R.; Donnely, T.; Lockhart, T. S. *Tetrahedron Lett*. **1985**, *26*, 359−362.
(5) Marcinek, A.; Platz, M. S.; Chan, S. Y.; Floresca, R.; Rajagopalan, K.; Golinski, M.; Watt, D. *J. Phys. Chem.* **1994**, *98*, 412−419.
(6) Kayama, R.; Hasunuma, S.; Sekiguchi, S.; Matsui, K. *Bull. Chem. Soc. Jpn*. **1974**, *47*, 2825−2829.
(7) Kayama, R.; Shizuka, H.; Sekiguchi, S.; Matsui, K. *Bull. Chem. Soc. Jpn*. **1975**, *48*, 3309−3312.
(8) Chapyshev, S. V. *Mendereev Commun.* **2003**, 43−55.
(9) Chapyshev, S. V.; Walton, R.; Sanborn, J. A.; Lahti, P. M. *J. Am. Chem. Soc.* **2000**, *122*, 1580−1588.
(10) Moriarty, R. M.; Rahman, M.; King, G. J. *J. Am. Chem. Soc.* **1966**, *88*, 842−843.
(11) Nakai, T.; Sato, K.; Shimoi, D.; Takui, T.; Itoh, K.; Kozaki, M.; Okada, K. *Mol. Cryst. Liq. Cryst.* **1999**, *334*, 157−166.
(12) Sato, T.; Narazaki, A.; Kawaguchi, Y.; Niino, H.; Bucher, G. *Angew. Chem., Int. Ed.* **2003**, *42*, 5206−5209.

10.1021/ja031794v CCC: $27.50

an aqueous solution of sodium azide according to the reported procedure.[13] The triazide **1** was photolyzed in a nitrogen matrix at 20 K.

Warning: 2,4,6-Triazido-1,3,5-triazine is a shock-sensitive and thermally unstable solid and should be handled with the precautions normally afforded to similar, potentially explosive materials.

Crystallites of **1** were vaporized at 40−45 °C and co-deposited with nitrogen (99.9999%) onto a CsI substrate at 20 K. Matrix-isolated **1** was photolyzed by using fourth-harmonic-generated (FHG) pulses from a Nd:YAG laser ($\lambda = 266$ nm, 10 Hz, 0.5 mJ·cm^{-2} pulse^{-1}; Lotis LS-2125 equipped with YHG-34). The sample chamber had a pair of quartz windows for UV−vis measurements and a pair of KBr windows for FTIR measurements, enabling us to monitor the photolysis by FTIR and UV−vis absorption spectroscopy simultaneously. The FTIR measurements were carried out on a PerkinElmer Spectrum GXI spectrometer with a resolution of 1 cm^{-1}. UV−vis absorption spectra were measured with a Shimadzu UV-3100 spectrometer.

II. Matrix Photolysis: EPR Measurement. X-band EPR spectra were recorded with a Bruker Elexsys E500 EPR spectrometer with an ER077R magnet (75 mm pole cap distance), an ER047 XG-T microwave bridge, and an oxygen-free high-conductivity copper rod (75 mm length, 2 mm diameter) cooled by an APD HC-2 closed-cycle cryostat, a vacuum shroud equipped with a sample inlet valve and a quartz window at the sides, a half-closed quartz tube (75 mm length, 10 mm diameter) at the bottom, and a vacuum pump system with a Pfeiffer Vacuum TMU071P turbo pump backed by a Leybold two-stage, rotary-vane pump. To avoid contamination of the high-vacuum segment by pump oil from the backing pump, a catalytic oxidation filter was placed between the rotary-vane pump and the turbo pump. During deposition and irradiation, the inlet port and the quartz window were positioned at the same height as the tip of the copper rod. For the measurement of the EPR spectra, the copper rod was lowered into the quartz tube at the bottom of the shroud, and the whole apparatus was moved downward so that the quartz tube and copper rod were positioned inside the EPR cavity.

Triazide **1** was evaporated at 30 °C and co-deposited with a large excess of argon (Messer-Griesheim, 99.9999%) on the tip of the copper rod at 13 K. The matrix-isolated sample was subsequently irradiated with a Gräntzel low-pressure mercury lamp (254 nm), and spectra were recorded at various irradiation times.

The computer simulation of the EPR spectrum was performed by using the Xsophe computer simulation software suite (version 1.0.4),[14] developed by the Centre for Magnetic Resonance and Department of Mathematics, University of Queensland, Brisbane (Australia) and Bruker Analytik GmbH, Rheinstetten (Germany). The simulation was performed by using a matrix diagonalization method for $S = 3$ and setting the parameter $\nu = 9.53125$ GHz and $g = 2.003$.

III. Computational Methods. All density functional theory (DFT) calculations were performed with the Gaussian 98 program package.[15] The geometries of the compounds were optimized by using the B3LYP method[16,17] in combination with the 6-31G* or cc-pVTZ basis set. The nature of the stationary points was assessed by means of vibrational frequency analysis. None of the optimized structures showed imaginary frequencies. Theoretical IR spectra were obtained by vibrational frequency analyses. Vibrational frequencies predicted at the B3LYP/6-31G* level were scaled by 0.9614, on the basis of the literature.[18] Calculated IR spectra were prepared by applying Gaussian peaks with 3 cm^{-1} full width at half-maximum for all bands. Calculations were done on the TACC Quantum Chemistry Grid/Gaussian Portal system at the Tsukuba Advanced Computing Center (TACC) and on a Hewlett-Packard Superdome 32000 located at Bochum.

Scheme 1. Reactive Species Generated Sequentially in the Photolysis of **1**

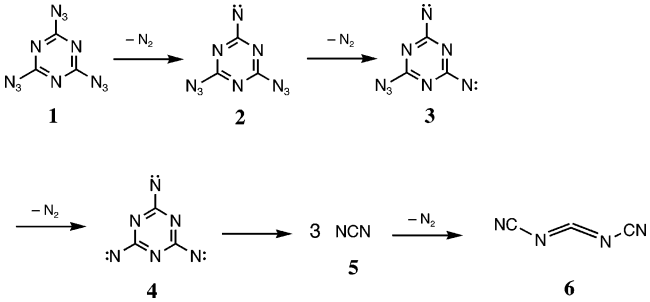

Results and Discussion

I. Matrix Photolysis: FTIR and UV−Vis Measurement. As discussed in our previous Communication,[12] five species were sequentially generated by the photolysis of **1** (Scheme 1). This result was clarified by the analysis of the dynamic behavior of the representative IR and UV−vis absorption bands (Figure 1). In this Article, we describe in detail the identification of the five species, based on a comparison of the observed IR bands and the DFT computational results.

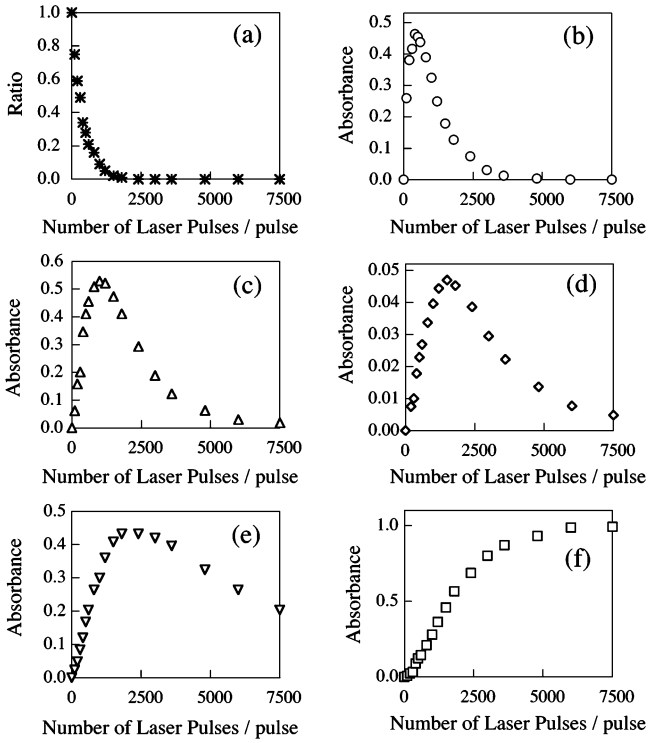

Figure 1. The dynamic behavior of representative IR and UV−vis bands of sequentially generated species. (a) **1**: Survival ratio against the initial amount of **1**. (b) **2**: IR band at 1339 cm^{-1}. (c) **3**: IR band at 1438 cm^{-1}. (d) **4**: IR band at 1326 cm^{-1}. (e) **5**: UV−vis band at 329 nm. (f) **6**: IR band at 2271 cm^{-1}.

(13) Ott, E.; Ohse, E. *Ber. Dtsch. Chem. Ges.* **1921**, *54*, 179−186.
(14) Griffin, M.; Muys, A.; Noble, C.; Wang, D.; Eldershaw, C.; Gates, K. E.; Burrage, K.; Hanson, G. R. *Mol. Phys. Rep.* **1999**, *26*, 60−84.
(15) Frisch, M. J.; Trucks, G. W.; Schlegel, H. B.; Scuseria, G. E.; Robb, M. A.; Cheeseman, J. R.; Zakrzewski, V. G.; Montgomery, J. A., Jr.; Stratmann, R. E.; Burant, J. C.; Dapprich, S.; Millam, J. M.; Daniels, A. D.; Kudin, K. N.; Strain, M. C.; Farkas, O.; Tomasi, J.; Barone, V.; Cossi, M.; Cammi, R.; Mennucci, B.; Pomelli, C.; Adamo, C.; Clifford, S.; Ochterski, J.; Petersson, G. A.; Ayala, P. Y.; Cui, Q.; Morokuma, K.; Malick, D. K.; Rabuck, A. D.; Raghavachari, K.; Foresman, J. B.; Cioslowski, J.; Ortiz, J. V.; Baboul, A. G.; Stefanov, B. B.; Liu, G.; Liashenko, A.; Piskorz, P.; Komaromi, I.; Gomperts, R.; Martin, R. L.; Fox, D. J.; Keith, T.; Al-Laham, M. A.; Peng, C. Y.; Nanayakkara, A.; Gonzalez, C.; Challacombe, M.; Gill, P. M. W.; Johnson, B.; Chen, W.; Wong, M. W.; Andres, J. L.; Gonzalez, C.; Head-Gordon, M.; Replogle, E. S.; Pople, J. A. *Gaussian 98*, Revision A.9; Gaussian, Inc.: Pittsburgh, PA, 1998.
(16) Becke, A. D. *J. Chem. Phys.* **1993**, *98*, 5648−5652.
(17) Lee, C.; Yang, W.; Parr, R. G. *Phys. Rev. B: Condens. Matter Mater. Phys.* **1988**, *37*, 785−789.

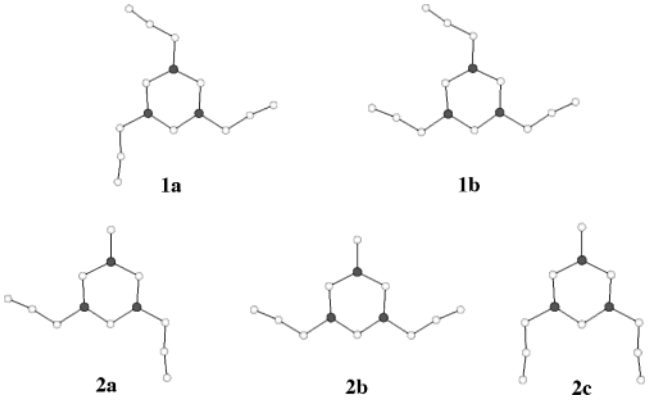

Figure 2. Optimized structures of **1** and **2** (B3LYP/6-31G* level).

The first intermediate generated was identified as the mononitrene **2**. This mononitrene could exist in the matrix as three different conformers **2a**−**2c**, reflecting the initial distribution of conformers **1a** and **1b** (Figure 2) in the matrix. The isomer **1a** was estimated to be 0.48 kcal·mol^{-1} more stable than **1b** at the B3LYP/6-31G* level. Whereas only isomer **2a** can be formed upon release of one nitrogen molecule from **1a**, the three isomers **2a**−**2c** should be formed from **1b** with equal probabilities. Therefore, the isomer **2a** should be formed with the highest probability. In terms of enthalpy, the differences between the three isomers are predicted to be negligible. If **1a** and **1b** are deposited in thermal equilibrium, and if all azide groups can undergo photocleavage with equal quantum yield, two-thirds of the mononitrene **2** generated would thus be in the form of **2a**, whereas **2b** and **2c** would each constitute only one-sixth of the mononitrene conformer mixture.

The representative IR band ascribed to **2** was observed at 1339 cm^{-1}. Although the three isomers should all exhibit intense bands at around 1339 cm^{-1}, they were predicted to have slightly different IR band patterns (Figure 3a−c). IR bands showing similar dynamic behavior were assigned to individual conformers (Figure 3e). The complex experimental IR spectrum indicated that the isomers coexisted in the matrix. With the exception of the azide-stretching band (ν_{N3}), the predicted IR bands of the isomers (Figure 3d) corresponded well with the observed IR bands. Although intense IR bands at around 2200 cm^{-1} were predicted for **2a**−**2c**, we found no such intense IR band there. We assigned two IR bands observed at around 2200 cm^{-1} to ν_{N3}. Intense ν_{N3} band should be split into these bands probably due to Fermi resonance.[19] On the basis of the earlier results on **1**,[11] benzene-triazide derivatives,[9,20] and triazine-azide derivatives,[21] the generated mononitrene **2** is expected to have a triplet ground state. Indeed, we observed the EPR signal ascribable to a triplet nitrene at around 8000 G (as we will discuss later). Given an earlier report on the formation of a seven-membered ring in a similar system,[21] mononitrene **2** could rearrange into a cyclic carbodiimide, which shows a characteristic IR band at around 1900 cm^{-1}. In the present case, we could observe only a weak IR band at around 1900 cm^{-1}, indicating that the rearrangement to a cyclic carbodiimide was a minor process in the present photolysis.[22] In addition to these IR bands, the UV−vis absorption band at 344 nm was also assigned to mononitrene **2**, on the basis of its dynamic behavior (Figure 4). Moreover, a broad band was observed at 460−640 nm. Chapyshev observed the broad absorption bands ascribable to triplet nitrene, quintet dinitrene, and septet trinitrene species in this wavelength region.[23] The dynamic behavior of this band implied that it could be ascribed to nitrene species **2**, **3**, or **4**, although we could not distinguish the bands produced by these species.

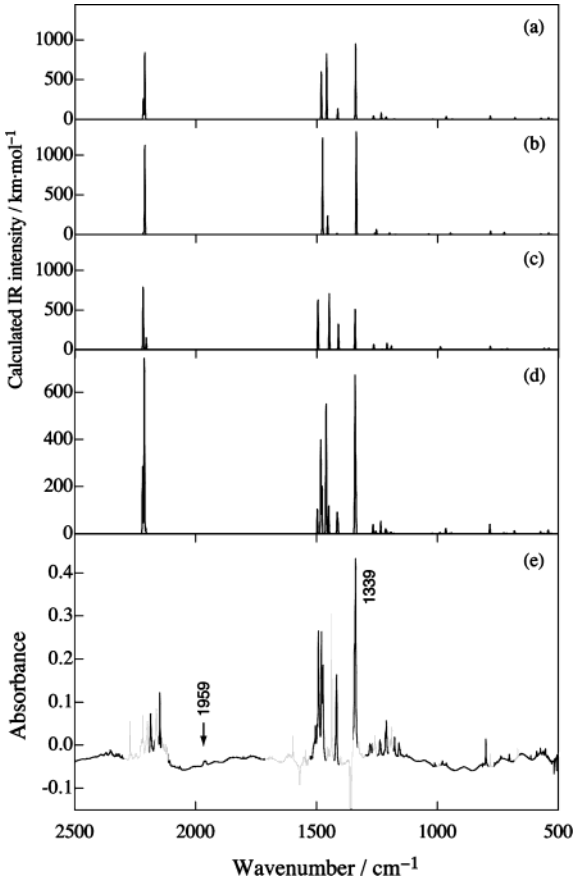

Figure 3. (a−c) Calculated IR spectra of three isomers **2a**−**2c**. (d) Calculated IR bands of a mixture of isomers of **2** (**2a**, 67%; **2b**, 17%; **2c**, 17%). (e) Observed IR bands ascribable to **2** selected on the basis of their dynamic behavior (similar to that of the band at 1339 cm^{-1}).

Upon further loss of nitrogen, the second intermediate, dinitrene **3**, should be formed. Dinitrene **3** showed an intense IR peak at 1438 cm^{-1}. Photolysis of all three isomers **2a**−**2c** should lead to the same dinitrene species. Therefore, the IR spectra should become simpler. IR bands showing a dynamic behavior similar to that of the band at 1438 cm^{-1} are shown in Figure 5. The IR spectrum assigned to **3** is simpler than that of **2**. The agreement between the experimental IR bands ascribed to **3** and the calculated spectrum is good, although a splitting

(18) Scott, A. P.; Radom, L. *J. Phys. Chem.* **1996**, *100*, 16502−16513.
(19) Four IR bands (2107, 2141, 2148, 2187 cm^{-1}) were assigned to mononitrene. On the other hand, IR bands of ν_{N3} were predicted at 2212.2 and 2218.3 cm^{-1} (**2a**), 2212.0 and 2217.5 cm^{-1} (**2b**), 2205.6 and 2219.0 cm^{-1} (**2c**). There were 10 possible combinations for **2a**, 15 possible combinations for **2b**, and 11 possible combinations for **2c** in the wavenumber region between 2100 and 2220 cm^{-1}.
(20) Chapyshev, S. V.; Kuhn, A.; Wong, M. W.; Wentrup, C. *J. Am. Chem. Soc.* **2000**, *122*, 1572−1579.
(21) Bucher, G.; Siegler, F.; Wolff, J. J. *Chem. Commun.* **1999**, 2113−2114.
(22) Intensity of the IR band at 1959 cm^{-1} was 2% of that of the IR band at1339 cm^{-1}, when the band (1339 cm^{-1}) was in its maximum. Calculated IR spectra of three isomers of the compounds with seven-membered ring, which might be formed by ring-expansion of nitrenes, are shown with the observed IR spectra in the Supporting Information.
(23) Chapyshev, S. V. *Mendereev Commun.* **2002**, 168−170.

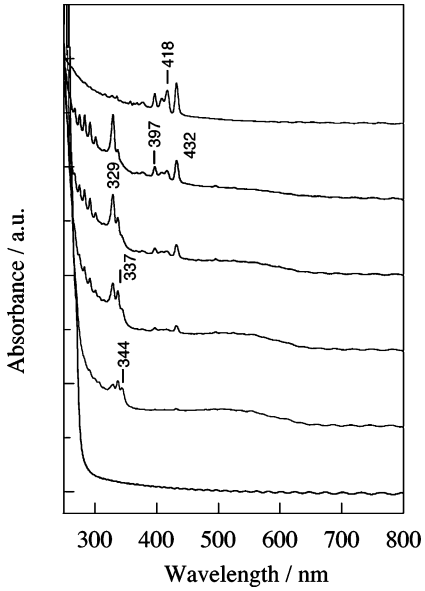

Figure 4. UV−vis absorption spectra of a nitrogen matrix containing **1** upon 266-nm irradiation with (bottom to top) 0, 400, 100, 1500, 2400, and 21 000 FHG pulses from a Nd:YAG laser.

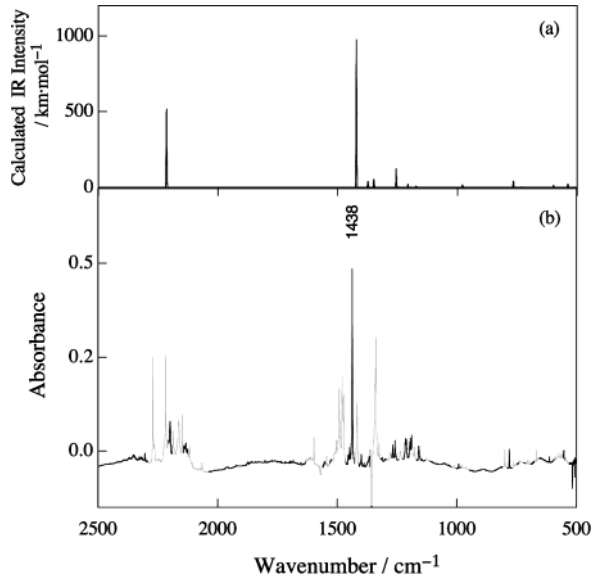

Figure 5. (a) Calculated IR spectrum of dinitrene **3** (B3LYP/6-31G* level). (b) Observed IR bands ascribed to **3** (selected on the basis of their dynamic behavior, which is similar to that of the band at 1438 cm^{-1}).

of the azide band was also observed here. Moreover, a UV−vis absorption band at 377 nm was ascribed to dinitrene **3** (Figure 4).

We have already discussed the identification of trinitrene **4** with the aid of isotopic labeling with ^{13}C.[12] We have thus identified **4** on the basis of two IR bands at 763 and 1326 cm^{-1}. The observed and calculated IR spectra are shown in Figure 6. The trinitrene should have a septet ground state. The septet species was not observed during the earlier photolysis of single-crystalline **1** at cryogenic temperatures.[5] In that experiment, the generated trinitrene **4** was surrounded by the unreacted triazide or the nitrene or dinitrene. The generated trinitrene **4** would readily react with these species, even at cryogenic temperatures. Such intermolecular reactions could be the reason **4** was not observed in the experiment with single-crystalline **1**. Intermolecular reactions can completely be ruled out if an argon matrix

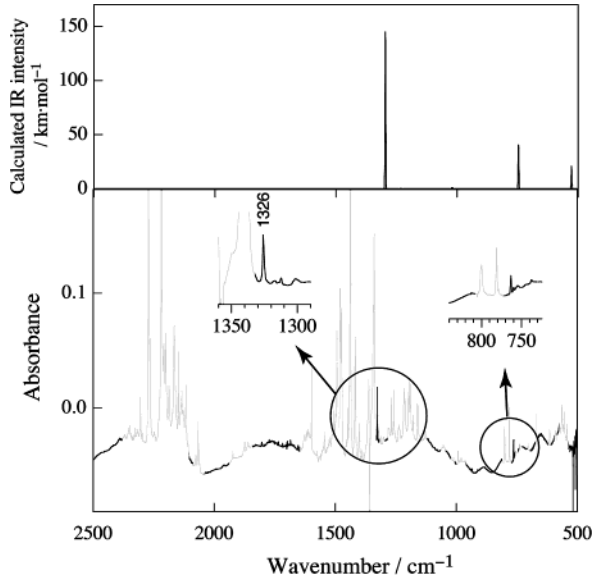

Figure 6. (a) Calculated IR spectra of trinitrene **4**. (b) Observed IR bands assigned to **4**, selected on the basis of their dynamic behavior similar to that of the band at 1326 cm^{-1}.

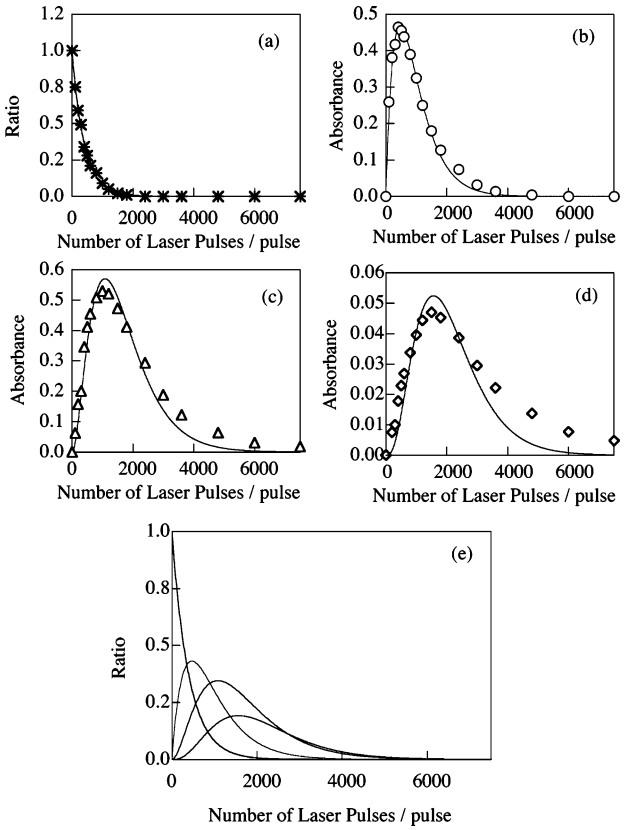

Figure 7. Dynamic behavior of the intensities of the IR bands of (a) **1**, (b) **2**, (c) **3**, and (d) **4** (symbols) and the result of the curve fitting using eqs 1, 2, 3, and 4 (solid curves). The estimated ratios of **1**, **2**, **3**, and **4** are shown in (e).

is employed. The major decomposition pathway of **4** was identified to be fragmentation into three NCN molecules.[12] This fragmentation was already suggested in an early EPR study as previously described.[10] We could observed EPR signals ascribable to both septet trinitrene **4** and triplet NCN molecule, as discussed later.

We have previously shown that apparently successive reactions proceeding in a matrix can be analyzed by applying kinetic equations.[24] This analysis provides quantitative information on the generated intermediates. We analyzed the curves shown in Figure 1 by assuming the successive reactions depicted in Scheme 1. Equations 1−4 were applied to a nonlinear least-squares fitting of the observed intensity changes for **1**, **2**, **3**, and **4**, respectively. **A**, **B**, **C**, **D**, and **E** denote triazide **1**, mononitrene **2**, dinitrene **3**, trinitrene **4**, and three NCN molecules, respectively. The results of the curve fittings are shown in Figure 7. The apparent rate constants were estimated to be $k_1 = 2.51 \times 10^{-4}$, $k_2 = 1.79 \times 10^{-4}$, $k_3 = 1.41 \times 10^{-4}$, and $k_4 = 2.19 \times 10^{-4}$ pulse^{-1}.

$$\mathbf{A} \xrightarrow{k_1} \mathbf{B} \xrightarrow{k_2} \mathbf{C} \xrightarrow{k_3} \mathbf{D} \xrightarrow{k_4} \mathbf{E} \rightarrow \ldots$$

$$[A] = [A]_0 \exp(-k_1 t) \quad (1)$$

$$[B] = \frac{k_1}{k_2 - k_1}\{\exp(-k_1 t) - \exp(-k_2 t)\}[A]_0 \quad (2)$$

$$[C] = \left\{\frac{k_1 k_2}{(k_2 - k_1)(k_3 - k_1)} \exp(-k_1 t) + \frac{k_1 k_2}{(k_1 - k_2)(k_3 - k_2)} \exp(-k_2 t) + \frac{k_1 k_2}{(k_1 - k_3)(k_2 - k_3)} \exp(-k_3 t)\right\}[A]_0 \quad (3)$$

$$[D] = \left\{\frac{k_1 k_2 k_3}{(k_2 - k_1)(k_3 - k_1)(k_4 - k_1)} \exp(-k_1 t) + \frac{k_1 k_2 k_3}{(k_1 - k_2)(k_3 - k_2)(k_4 - k_2)} \exp(-k_2 t) + \frac{k_1 k_2 k_3}{(k_1 - k_3)(k_2 - k_3)(k_4 - k_3)} \exp(-k_3 t) + \frac{k_1 k_2 k_3}{(k_1 - k_4)(k_2 - k_4)(k_3 - k_4)} \exp(-k_4 t)\right\}[A]_0 \quad (4)$$

The intensity changes for **1** and **2** were well reproduced by the fitted curves obtained from eqs 1 and 2 (Figure 7a,b). On the other hand, the deviation between the observed intensities and the curve-fitting result increased for **3** and **4**. This deviation indicated that the photochemical reaction from **1** to **4** was not a successive reaction. This is probably attributable to the existence of minor side reactions, such as the formation of the cyclic carbodiimide. By assuming that this deviation was reasonably small, we could roughly estimate the ratio of the intermediates in the matrix (Figure 7e). From this analysis, the relative concentration of trinitrene **4** reached a maximum (19%) when 98% of **1** was photolyzed. At the same time, the relative concentrations of **2** and **3** were estimated to be 14% and 30%, respectively.

II. Matrix Photolysis: EPR Measurement. The EPR spectra observed upon 254-nm irradiation of **1** are shown in Figure 8. Initially, an EPR signal ascribable to a triplet nitrene appeared at around 8000 G (Figure 8a). This signal is a typical EPR signal for a mononitrene species.[25] In the present study, D and E values

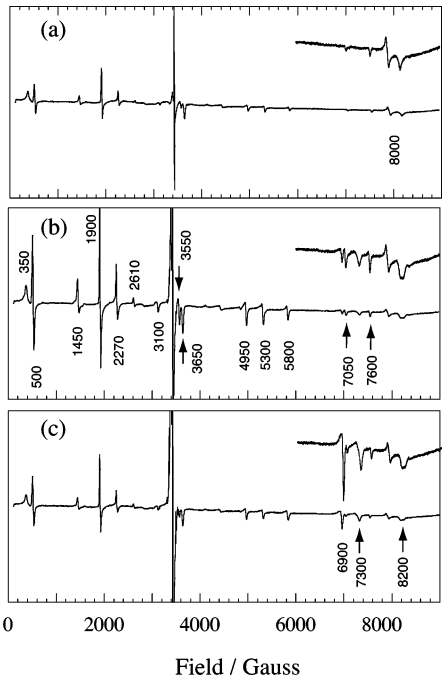

Figure 8. EPR spectra of an argon matrix containing **1** upon irradiation at 254 nm for (a) 2 min, (b) 10 min, and (c) 40 min.

for this signal were obtained as a best fit for $D = 1.461$ and $E = 0.005$ cm^{-1} ($g = 2.003$), respectively. A similar signal was also observed in the earlier EPR study on **1**:[11] The fine-structure D and E values were preliminary estimated as $D = 1.445$ and $E = 0.0045$ cm^{-1}, respectively, by the powder-pattern EPR measurement. These values were in fair agreement with the values estimated in the present study and in the earlier study.[10] Meanwhile, the preliminary parameters were determined as $D = 1.402$ and $E = 0.011$ cm^{-1}, respectively, by the single-crystal EPR measurement.[11] While the signal ascribed to mononitrene decreased, other signals increased upon the prolonged irradiation (Figure 8b).

As in the case of FTIR and UV−vis spectra, the fact that the signals appeared sequentially indicated that the photoreactions proceeded in a stepwise manner in the matrix. The observed EPR signals can be grouped, as in the case of the FTIR and UV−vis bands (Figure 9). It should be noted that the time profile for the FTIR and UV−vis bands could be different because of differences in experimental conditions, such as the thickness of the matrix and the irradiation conditions. Accordingly, the dynamic behavior of EPR signals does not fully correspond with that of FTIR or UV−vis bands. For instance, IR bands ascribed to nitrene species showed maximum intensity upon laser irradiation ($\lambda = 266$ nm) with 400 pulses and then completely disappeared upon irradiation with ca. 5000 pulses (Figure 1b). In contrast, the intensity of the EPR signal assigned to **2** reached a photostationary state at approximately one-half of the maximum intensity (Figure 9a). This discrepancy could arise from differences in filtering effects related to the different thicknesses of the matrixes in the EPR experiments as compared to the IR and UV−vis measurements or it could be caused by the different excitation conditions used (Nd:YAG laser vs a Hg low-pressure lamp). When the matrix was made thicker in the IR experiment,

(24) Sato, T.; Arulmozhiraja, S.; Niino, H.; Sasaki, S.; Matsuura, T.; Yabe, A. *J. Am. Chem. Soc.* **2002**, *124*, 4512−4521.

(25) Wasserman, E. *Prog. Phys. Org. Chem.* **1971**, *8*, 319−336.

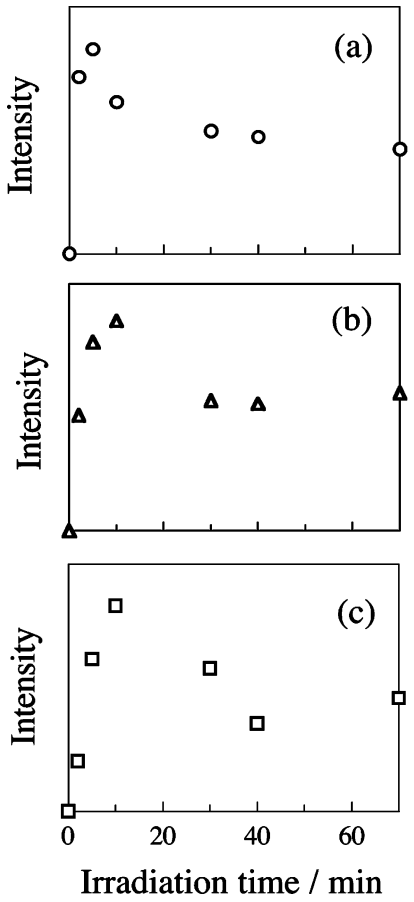

Figure 9. Dynamic behavior of representative EPR signals: (a) 8000 G, (b) 350 G, and (c) 500 G.

it proved to be impossible to photolyze **1** to completion, even if more-intense laser irradiation was applied.

The signal ascribable to mononitrene **2** increased during the initial irradiation and then decreased (Figure 9a). In turn, several new signals increased, as indicated in Figure 8b: these signals could be ascribed to the dinitrene or trinitrene. Among these signals, those observed at 350 and 500 G showed a slightly different dynamic behavior, indicating that two species were generated (Figure 9b,c). The signals observed at 350 and 3650 G were ascribed to the second intermediate, which should be dinitrene **3**. On the other hand, signals that showed similar dynamic behaviors to that at 500 G are shown in Figure 10 (bottom). These signals could be assigned to the third intermediate, trinitrene **4**.

The simulation of the EPR spectrum of trinitrene **4** was performed by using a matrix diagonalization method for $S = 3$ and by setting the parameters $\nu = 9.53125$ GHz and $g = 2.003$. Figure 10 (top) shows the simulated EPR spectrum with $S = 3$, $g = 2.003$, $D = 0.123$ cm^{-1}, and $E = 0.000$ cm^{-1}. Signals appearing in the simulated spectra agreed perfectly with the experimental EPR signals assigned to trinitrene **4**. Thus, we could confirm that the generated trinitrene **4** possessed the septet ground state. There is very little precedent for interpreting the EPR spectra of systems with three nitrene units attached to a single conjugated ring system. Wasserman, Schueller, and Yager reported on an EPR spectroscopic study on 1,3,5-tricyanophenyltrinitrene.[26] They assigned ESR peaks at 420, 1650, and 2750 G to the trinitrene and estimated the D values as 0.0674 cm^{-1}, but they did not report the spectra. Chapyshev et al. recently

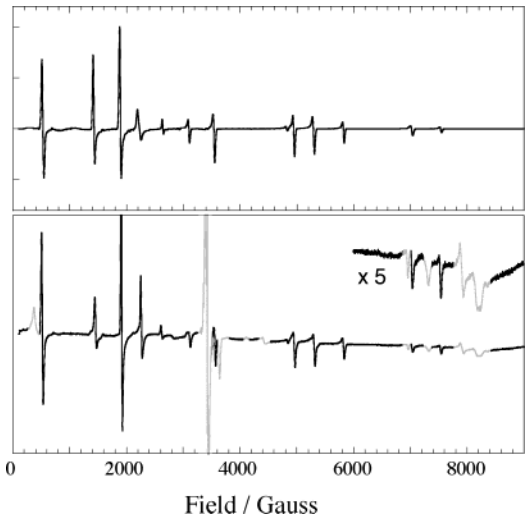

Figure 10. (Top) Simulated EPR spectrum with $S = 3$, $g = 2.003$, $D = 0.123$ cm^{-1}, $E = 0.000$ cm^{-1}. (Bottom) Experimental EPR signals assigned to trinitrene **4**. These signals showed a similar time dependence to that of the signal at 500 G (Figure 9c).

reported on the septet trinitrenes generated by the photolysis of 3,5-dichloro-2,4,6-triazidopyridine and 3-chloro-5-cyano-2,4,6-triazidopyridine.[3] In their work, they estimated that $D \approx 0.1$ cm^{-1}, with small E values for both trinitrene species.

Complex EPR spectra for randomly oriented high-spin multiplicity systems have been simulated by the eigenfield-based calculation.[27−30] On the other hand, the fine-structure parameters of oligonitrenes could be reproduced by a semiempirical calculation of the fine-structure tensor by eq 5.[31] This calculation reproduced fine-structure parameters of septet trinitrene[32] as well as quintet dinitrenes.[9,11,33,34] ρ_k and ρ_{mono} were spin densities

$$\mathbf{D} = [S(2S-1)]^{-1}\sum_k \left(\frac{\rho_k}{\rho_{\mathrm{mono}}}\right) \cdot \mathbf{U}_k \mathbf{d}_{\mathrm{mono}} \mathbf{U}_k^{\dagger} \qquad (5)$$

on nitrene moieties in septet trinitrene and triplet mononitrene. The septet trinitrene optimized at the UB3LYP/6-31G* level had a D_{3h} symmetrical structure. Therefore, angles between two C−N bonds in nitrene moieties were 120° and spin densities of three nitrene moieties were estimated as $\rho_k = 1.723$. Three isomers of the mononitrene showed spin densities of 1.772, 1.769, 1.775, respectively. The averaged value $\rho_{\mathrm{mono}} = 1.772$ was applied to eq 5. From the parameters ($D = 1.461$ cm^{-1} and $E = 0.005$ cm^{-1}) of triplet mononitrene estimated in the present study, the parameters for the septet trinitrene were calculated to be $D = -0.146$ and $E = 0.00$ cm^{-1}. The estimated D value was larger than the experimental value ($D = 0.123$ cm^{-1}). The D and E values of triplet mononitrene were close

(26) Wasserman, E.; Schueller, K.; Yager, W. A. *Chem. Phys. Lett.* **1968**, *2*, 259−260.
(27) Belford, G. G.; Belford, R. L.; Burkhalter, J. F. *J. Magn. Reson.* **1973**, *11*, 251−262.
(28) Teki, Y.; Takui, T.; Yagi, H.; Itoh, K.; Iwamura, H. *J. Chem. Phys.* **1985**, *83*, 539−547.
(29) Teki, Y.; Fujita, I.; Takui, T.; Kinoshita, T.; Itoh, K. *J. Am. Chem. Soc.* **1994**, *116*, 11499−11505.
(30) Sato, K., Ph.D. Thesis, Osaka City University, Osaka, Japan, 1994.
(31) Teki, Y.; Takui, T.; Itoh, K.; Iwamura, H.; Kobayashi, K. *J. Am. Chem. Soc.* **1986**, *108*, 2147−2156.
(32) Oda, N.; Nakai, T.; Sato, K.; Shimoi, D.; Kozaki, M.; Okada, K.; Takui, T. *Synth. Met.* **2001**, *121*, 1480−1481.
(33) Kalgutkar, R. S.; Lahti, P. M. *J. Am. Chem. Soc.* **1986**, *108*, 2147−2156.
(34) Kalgutkar, R. S.; Lahti, P. M. *Tetrahedron Lett.* **2003**, *44*, 2625−2628.

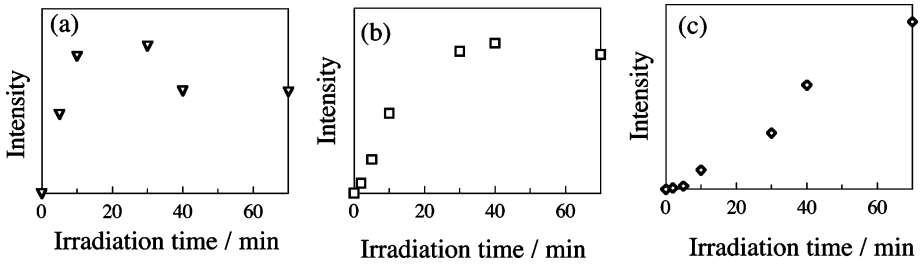

Figure 11. Dynamic behavior of the representative EPR signals: (a) 8200 G, (b) 7300 G, and (c) 6900 G.

to the values estimated by powder-pattern EPR measurement. By using the parameters determined by single-crystal EPR measurement, the calculated parameters were $D = -0.133$ cm^{-1} and $E = 0.000$ cm^{-1}. Thus, the agreement between calculated parameters and experimental values was improved. These results revealed that the estimated D value of **4**, which was larger than that obtained by Chapyshev et al.,[9] was mainly based on the larger D value of **2** compared to that of phenyl nitrene.

The disappearance of the signals assigned to **3** and **4** was accompanied by a growth of the signals at around 8200, 7300, and 6900 G (Figure 8c). These signals could be ascribed to products of the photochemical reaction of trinitrene **4**. On the basis of its characteristic UV−vis bands, we confirmed that trinitrene **4** photochemically decomposed into three molecules of NCN upon prolonged irradiation.[35] This should be the main decomposition pathway of matrix-isolated **4**. NCN thus generated would be in the triplet ground state. NCN has been reported to rearrange photochemically to triplet CNN,[35−37]whose EPR spectrum was reported by Wasserman et al.[25,38] The reported D and E values for NCN were 1.544 and <0.002 cm^{-1}, respectively, whereas those for CNN were 1.153 and <0.002 cm^{-1}, respectively. Simulations based on these values revealed that the EPR signal observed at around 8200 G could be ascribed to triplet NCN. In the present study, D and E values of NCN were determined by simulation as 1.545 and 0.000 cm^{-1}, respectively. On the other hand, a signal for CNN was predicted to appear at around 7300 G. The D and E values of CNN were determined by simulation as 1.153 and 0.000 cm^{-1}, respectively. In our EPR experiments, a signal at 8200 G appeared after the decomposition of septet trinitrene **4**, and later, a signal at around 7300 G appeared (Figure 11a,b).

Triplet CNN has been reported to show an IR band at 1241 cm^{-1} upon further photoirradiation.[36] We could detect a very weak IR band appearing at 1233 cm^{-1} when the population of NCN had reached its maximum. This IR band might be attributable to CNN. The band was very weak, whereas the EPR signal for CNN was easily discernible. It is probable that EPR spectroscopy is more sensitive than IR spectroscopy for the detection of CNN. The final EPR signal, observed at around 6900 G, has not been identified. Given the reported fate of NCN intermediates, this signal could originate from a reaction product derived from triplet atomic carbon.[35,39] Finally, the UV−vis bands observed at 397, 418, and 432 nm could not be attributed to *N*,*N*′-dicyanocarbodiimide **6**. The unidentified species responsible for these UV−vis bands might be the source of the EPR signal.

Conclusion

We studied the photochemistry of 2,4,6-triazido-1,3,5-triazine in a nitrogen matrix at 20 K. In this photolysis, the sequential generation of the mononitrene, dinitrene, and trinitrene was observed. The generation of 2,4,6-trinitreno-1,3,5-triazine was confirmed for the first time by both matrix IR and EPR spectroscopy. In particular, EPR spectra revealed that the trinitrene generated was in its septet ground state. Trinitrene **4** readily decomposed into three NCN molecules upon further photoirradiation. By matrix EPR spectroscopy, we were able to observe the generation of triplet NCN and CNN, concomitant with the decay of trinitrene **4**.

Acknowledgment. T.S. acknowledges Prof. Curt Wentrup and Dr. Sergei Chapyshev for helpful information. This work was supported by the Fund of Support for Young Researchers with a Term, Ministry of Education, Culture, Sports, Science, and Technology, Japan. G.B. and W.S. acknowledge financial support by the Otto Röhm-Gedächtnisstiftung, the Fonds der Chemischen Industrie, and the Deutsche Forschungsgemeinschaft.

Supporting Information Available: Optimized geometries and vibrational frequencies of the calculated species. This material is available free of charge via the Internet at http://pubs.acs.org.

JA031794V

(35) Milligan, D. E.; Jacox, M. E.; Bass, A. M. *J. Chem. Phys.* **1965**, *43*, 3149−3160.
(36) Milligan, D. E.; Jacox, M. E. *J. Chem. Phys.* **1966**, *44*, 2850−2856.
(37) Maier, G.; Bothur, A.; Eckwert, J.; Reisenauer, H. P. *Chem.−Eur. J.* **1998**, *4*, 1964−1968.
(38) Wasserman, E.; Barash, L.; Yager, W. A. *J. Am. Chem. Soc.* **1965**, *87*, 2075−2076.
(39) Krogh, O. D.; Ward, C. H.; Hollenbeck, J. M. *J. Phys. Chem.* **1982**, *86*, 6, 2892−2895.